Does SHEM for Additive Schwarz work better than predicted by its condition number estimate ?

Petter E. Bjørstad[2], Martin J. Gander[1], Atle Loneland[2], and Talal Rahman[3]

1 Introduction and Model Problem

The SHEM (Spectral Harmonically Enriched Multiscale) coarse space is a new coarse space for arbitrary overlapping or non-overlapping domain decomposition methods. In contrast to recent new coarse spaces like GenEO [13] or the one in [12] that improve certain Rayleigh quotients in the convergence analysis of the underlying domain decomposition method, SHEM is based on understanding the stationary iterates of the domain decomposition method itself (see [6] for details), and can thus be constructed and used also for domain decomposition methods which do not (yet) have such a convergence analysis, like for example Restricted Additive Schwarz (RAS) [7], or optimized Schwarz [4]. SHEM is based on the approximation of an optimal coarse space which was discovered in [3], and further studied in [5, 4, 7], see [6] for a general introduction, and also [9] for the specific case of Additive Schwarz (AS). SHEM can use spectral information, as its name indicates, but can also be constructed avoiding eigenvalue problems, for examples, see [8]. If a convergence analysis for the domain decomposition method is available, SHEM can improve the corresponding convergence estimate, see [8] for a condition number estimate when SHEM is used with AS. We are interested here to test numerically if in this case

1. the hypothesis of small overlap (one or two mesh sizes) in the proof in [9] is necessary for the condition number estimate to hold in practice;
2. the quadratic growth in the factor H/h in the condition number estimate from [9] is really present when the method is used numerically.

Section of Mathematics, University of Geneva, 1211 Geneva 4, Switzerland Martin.Gander@unige.ch · Department of Informatics, University of Bergen, 5020 Bergen, Norway Atle.Loneland@ii.uib.no · Department of Computing, Mathematics and Physics, Western Norway University of Applied Sciences, 5063 Bergen, Norway Talal.Rahman@hvl.no

We consider as our model problem the following variational formulation of a second order elliptic boundary value problem with Dirichlet boundary conditions: find $u \in H_0^1(\Omega)$ such that

$$a(u,v) = \int_\Omega \alpha(x)\nabla u \cdot \nabla v \, dx = \int_\Omega fv \, dx \quad \forall v \in H_0^1(\Omega), \tag{1}$$

where Ω is a bounded convex domain in $\mathbb{R}^2$, $f \in L^2(\Omega)$ and $\alpha \in L^\infty(\Omega)$ such that $\alpha \geq \alpha_0$ for some positive constant α_0. Discretizing this problem using P1 finite elements from the finite element space V_h with associated mesh $\mathcal{T}_h(\Omega)$ leads to the linear system

$$A\mathbf{u} = \mathbf{f}. \tag{2}$$

Let Ω be partitioned into non-overlapping open, connected Lipschitz polytopes $\{\Omega_i : i = 1, \ldots, N\}$ such that $\overline{\Omega} = \bigcup_{i=1}^N \overline{\Omega}_i$, where each $\overline{\Omega}_i$ is assumed to consist of elements from $\mathcal{T}_h(\Omega)$. We assume that this partitioning is shape-regular. By extending each subdomain Ω_i with a distance δ in each direction, we create a further decomposition of Ω into overlapping subdomains $\{\Omega_i'\}_{i=1}^N$. As usual, we assume that each point $x \in \Omega$ is contained in at most N_0 subdomains (finite covering). The layer of elements in Ω_i touching the boundary $\partial\Omega_i$ is denoted by Ω_i^h and we assume that the triangles corresponding to this layer are shape regular with minimum diameter $h_i := \min_{K \in \mathcal{T}_h(\Omega_i^h)} h_K$, where h_K is the diameter of the triangle K. The interfaces between two subdomains, Ω_i and Ω_j, are defined as $\overline{\Gamma}_{ij} := \overline{\Omega}_i \cap \overline{\Omega}_j$. The sets of vertices of elements in $\mathcal{T}_h(\Omega)$ (nodal points) belonging to Ω, Ω_i, $\partial\Omega$, $\partial\Omega_i$ and Γ_{ij} are denoted by Ω_h, Ω_{ih}, $\partial\Omega_h$, $\partial\Omega_{ih}$ and Γ_{ijh}. With each interface we define the space of finite element functions restricted to Γ_{ij} and zero on $\partial\Gamma_{ij}$ as $V_h^0(\Gamma_{ij})$.

We define the restriction of the bilinear form $a(\cdot,\cdot)$ to an interface Γ_{ij} shared by two subdomains as

$$a_{\Gamma_{ij}}(u,v) := \left(\alpha_{|\Gamma_{ij}}(x) D_\tau u, D_\tau v\right)_{L^2(\Gamma_{ij})},$$

where $\alpha_{|\Gamma_{ij}}(x) := \lim_{y \in \Omega_i \to x} \alpha(y)$ and D_τ denotes the tangent derivative with respect to Γ_{ij}. In order to obtain continuous basis functions across subdomain interfaces, we define a second bilinear form on each interface Γ_{ij},

$$\bar{a}_{\Gamma_{ij}}(u,v) := \left(\overline{\alpha}_{ij}(x) D_\tau u, D_\tau v\right)_{L^2(\Gamma_{ij})},$$

where $\overline{\alpha}_{ij}$ is taken as the maximum of $\alpha_{|\Gamma_{ij}}$ and $\alpha_{|\Gamma_{ji}}$.

Given a partition of unity $\{\chi_i\}_{i=1}^N$ subordinate to the overlapping decomposition defined above and corresponding restriction matrices R_i, as well as a suitable coarse space V_0 with restriction operator R_0, the two-level additive Schwarz method may be defined for $i = 0, \ldots N$ as

$$M_{AS,2}^{-1} = \sum_{i=0}^{N} R_i^T A_i^{-1} R_i \qquad \text{where} \quad A_i := R_i A R_i^T. \tag{3}$$

Classically, coarse spaces for Additive Schwarz methods consist of finite elements on a coarser triangulation $\mathcal{T}_H$ of Ω. This type of choice for the coarse space, however, is not robust with respect to large variations in the coefficient α.

2 The SHEM Coarse Space

SHEM is based on enriching a particular underlying coarse space, which in the case of high contrast problems is the multiscale finite element coarse space, see [1, 10]. We use the variant that generates the multiscale elements by solving lower dimensional problems along the edges, and then extending the result harmonically into the interior of the element. In the case of Laplace's equation on a rectangular domain decomposition, this underlying coarse space would just be Q1 finite elements on the subdomains, see [5]. Note that SHEM is also interesting in this case, since it systematically improves the overall convergence of the underlying domain decomposition method in an optimized way, see [9]. We choose here for SHEM a harmonic enrichment based on solutions of local eigenvalue problems along the interfaces between subdomains[1]:

Definition 1 (Generalized Interface Eigenvalue Problem). For each interface Γ_{ij}, we define the generalized eigenvalue problem: find ψ and λ, such that

$$\bar{a}_{\Gamma_{ij}}(\psi, v) := \lambda b_{\Gamma_{ij}}(\psi, v) \qquad \forall v \in V_h^0(\Gamma_{ij}), \tag{4}$$

where $b_{\Gamma_{ij}}(\psi, v) := h_i^{-1} \sum_{k \in \Gamma_{ijh}} \beta_k \psi_k v_k$ and $\beta_k = \sum_{\substack{K \in \mathcal{T}_h(\Omega) \\ k \in \mathrm{dof}(K)}} \alpha_K$.

We will test the following two types of SHEM coarse spaces:

- SHEM$_m$, where m is an integer: here we choose the m eigenfunctions associated with the smallest m eigenvalues of (4), and extend each of them harmonically into the two subdomains Ω_i and Ω_j adjacent to the interface Γ_{ij} with zero Dirichlet boundary conditions on the remaining part of the subdomain boundaries. These functions are then added to the underlying multiscale coarse space to form SHEM$_m$.
- SHEM$_\tau$, where τ is a given tolerance: here we choose adaptively on each interface Γ_{ij} to include all eigenfunctions associates with eigenvalues smaller

[1] Any other Sturm Liuville problem could be used as well to get a different variant of SHEM, for example more expensive Schur complements corresponding to the Dirichlet to Neumann maps [11], or one could construct even cheaper interface basis functions without eigenvalue problem, see [8].

than τ, extend them harmonically like above and add them to the underlying multiscale coarse space to form SHEM_τ.

Theorem 1 (Condition Number Estimate [8]). *If the overlap is one or two mesh sizes, then the condition number of the two level Schwarz operator (3) with the SHEM_m coarse space can be bounded by*

$$\kappa(M_{AS,2}^{-1}A) \preceq C_0^2(N_0+1), \tag{5}$$

where $C_0^2 \simeq \left(1+\frac{1}{\lambda_{m+1}}\right)$ *and* $\lambda_{m+1} := \min_i \min_{\Gamma_{ij}\subset\partial\Omega_i} \lambda^{ij}_{m_{ij}+1}$.

The restriction on the overlap size is necessary in the proof based on the abstract Schwarz framework. The convergence estimate in Theorem 1 also indicates a quadratic dependence of the condition number on the mesh ratio H/h, even for the case without enrichment, because the inverse of the smallest eigenvalues of (4) have a quadratic dependence on the ratio H/h. In the case of Laplace's equation and without enrichment, such that our coarse space is just the normal Q1 coarse space, standard domain decomposition theory says that the condition number of additive Schwarz should depend linearly on the mesh ratio H/h. We investigate now numerically if these restrictions are really also properties of SHEM_m, or just artefacts in the analysis.

3 Numerical Investigation of the SHEM coarse space

We solve problem (1) with $f = 1$ on a unit square domain $\Omega = (0,1)^2$, and the coefficient $\alpha(x)$ represents various (possibly discontinuous) distributions. We use AS with SHEM_m as a preconditioner for the conjugate gradient method, and stop the iteration when the l_2 norm of the residual is reduced by a factor of 10^{-6}. If not stated otherwise, the coefficient $\alpha(x)$ is equal to 1 for all the numerical examples, except in the areas marked with red where the value of $\alpha(x)$ is equal to $\hat{\alpha}$. All the experiments were carried out using Matlab 9.0 on a serial workstation. For the interface eigenvalue problems, we have in our implementation exploited the fact that we are able to extract exactly the 1D stiffness and mass matrix corresponding to the bilinear forms in Definition 1 algebraically from the global problem.

3.1 Is small overlap necessary for SHEM?

We start by studying the dependence on the overlap for the contrast function $\alpha(x)$ shown in Figure 1. For the case of overlap $\delta = 2h$ and $\delta = 8h$, we show the iteration counts and condition number estimates in Table 1 for

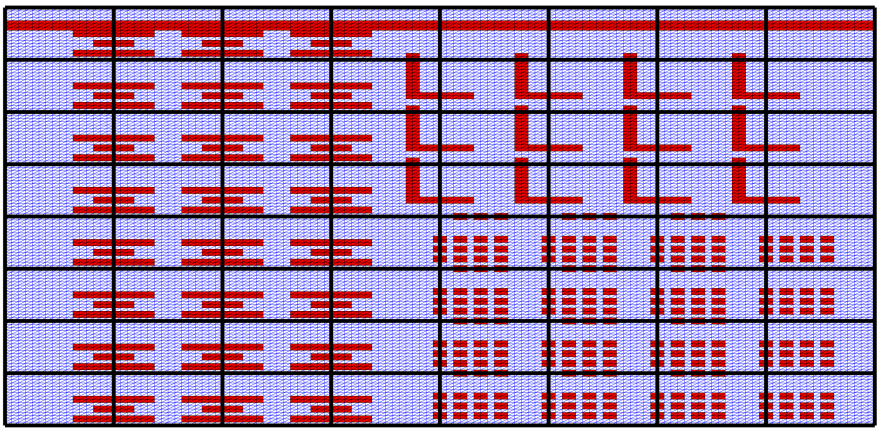

Fig. 1 Distribution of α for a geometry with $h = \frac{1}{128}$, $H = 16h$. The regions marked with red are where α has a large value $\hat{\alpha}$.

the classical multiscale coarse space (MS), SHEM$_m$ and the adaptive variant SHEM$_{\tau=6e-3}$. We see that even though the theory only addressed small overlap, SHEM$_m$ works very well also with larger overlap, and overlap improves the performance like usual. We even see that independence of the contrast arrives for the large overlap already with two enrichment functions instead of three. This is because the middle of the three channels crossing the interfaces in Figure 1 is shorter, and for the large overlap case included in the overlap, and thus not a convergence problem any more for the underlying AS; there are therefore only two channels left the coarse space has to treat, see [6] presented at this conference. In the current adaptive variant SHEM$_{\tau=6e-3}$ it is not clear how to take into account the overlap, and thus the same number of

	MS	SHEM$_1$	SHEM$_2$	SHEM$_3$	SHEM$_4$	SHEM$_{\tau=6e-3}$	
dim.	49	161	273	385	497		
$\hat{\alpha}$	#it. (κ)	#it. (κ)	#it. (κ)	#it. (κ)	#it. (κ)	#it. (κ)	dim.
10^0	21 (1.29e1)	16 (7.45e0)	15 (5.99e0)	13 (5.19e0)	13 (5.15e0)	21 (1.29e1)	49
10^2	122 (3.74e2)	70 (1.17e2)	47 (6.70e1)	19 (6.77e0)	16 (5.66e0)	25 (1.10e1)	233
10^4	367 (3.64e4)	248 (1.10e4)	187 (6.22e3)	19 (6.78e0)	17 (5.73e0)	25 (1.09e1)	233
10^6	610 (3.64e6)	423 (1.10e6)	290 (6.22e5)	19 (6.78e0)	17 (5.73e0)	25 (1.09e1)	233
10^0	16 (5.57e0)	15 (4,88e0)	15 (4.82e0)	15 (4.94e0)	15 (4.95e0)	16 (5.47e0)	49
10^2	47 (4.08e1)	28 (1.53e1)	19 (5.58e0)	18 (5.02e0)	18 (4.99e0)	21 (6.26e0)	233
10^4	145 (3.48e3)	55 (1.08e3)	20 (6.03e0)	18 (5.06e0)	18 (4.99e0)	21 (6.55e0)	233
10^6	241 (3.48e5)	78 (1.08e5)	20 (6.03e0)	18 (5.06e0)	18 (4.99e0)	21 (6.56e0)	233

Table 1 Top half: overlap $\delta = 2h$. Bottom half: overlap $\delta = 8h$. Iteration count and condition number estimate for the channel distribution in Figure 1 for the classical multiscale coarse space, SHEM$_m$, $m = 1, 2, 3, 4$ and SHEM$_{\tau=6e-3}$ for $h = \frac{1}{128}$, $H = 16h$. Here 'dim' denotes the dimension of the coarse space.

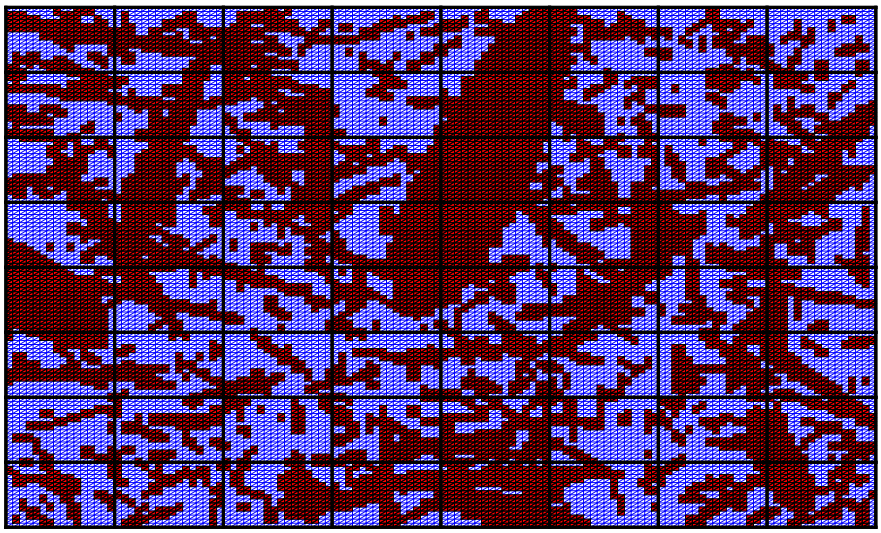

Fig. 2 Distribution of α for a geometry with $h = \frac{1}{128}$, $H = 16h$. The regions marked with red are where α has a large value $\hat{\alpha}$.

enrichment functions was chosen. Larger overlap can however also be taken into account by a different construction of SHEM for AS, see [9].

We next perform the same test also on the irregular high contrast structure shown in Figure 2. The corresponding results in Table 2 show that also in this case SHEM works very well with larger overlap, and that difficulties can be either remedied by increasing the overlap, or enriching the coarse space: SHEM with one enrichment function is enough to get robust convergence with large overlap, but with small overlap, SHEM needs 2-3 enrichment functions.

	MS	SHEM_1	SHEM_2	SHEM_3	SHEM_4	$\text{SHEM}_{\tau=6e-3}$	
dim.	49	161	273	385	497		
$\hat{\alpha}$	#it. (κ)	#it. (κ)	#it. (κ)	#it. (κ)	#it. (κ)	#it. (κ)	dim.
10^0	21 (1.29e1)	16 (7.45e0)	15 (5.99e0)	13 (5.19e0)	13 (5.15e0)	21 (1.29e1)	49
10^2	72 (1.09e2)	53 (6.49e1)	27 (1.52e1)	22 (9.47e0)	20 (6.45e0)	36 (2.14e1)	165
10^4	288 (9.43e3)	98 (5.46e3)	29 (1.60e1)	23 (9.60e0)	21 (6.54e0)	38 (2.44e1)	169
10^6	524 (9.41e6)	156 (5.49e5)	32 (1.60e1)	24 (9.59e0)	22 (6.28e0)	39 (2.44e1)	169
10^0	16 (5.57e0)	15 (4,88e0)	15 (4.82e0)	15 (4.94e0)	15 (4.95e0)	16 (5.47e0)	49
10^2	29 (1.31e1)	22 (7.75e0)	19 (5.54e0)	18 (5.10e0)	18 (5.05e0)	22 (7.89e0)	165
10^4	72 (7.56e2)	28 (1.36e1)	20 (5.68e0)	19 (5.12e0)	19 (5.07e0)	25 (9.97e0)	169
10^6	121 (7.50e4)	32 (1.43e2)	21 (5.41e0)	20 (5.05e0)	20 (5.02e0)	26 (1.01e1)	169

Table 2 Top half: overlap $\delta = 2h$. Bottom half: overlap $\delta = 8h$. Iteration count and condition number estimate for the distribution in Figure 2 for the classical multiscale coarse space, SHEM_m, $m = 1, 2, 3, 4$ and $\text{SHEM}_{\tau=6e-3}$ for $h = \frac{1}{128}$, $H = 16h$. Here 'dim' denotes the dimension of the coarse space.

	MS	SHEM_1	SHEM_2	SHEM_3	SHEM_4
$\frac{H}{h}$	#it. (κ)	#it. (κ)	#it. (κ)	#it. (κ)	#it. (κ)
8	18 (7.67e0)	14 (5.36e0)	14 (5.02e1)	14 (5.07e0)	13 (5.12e0)
16	21 (1.29e1)	16 (7.45e0)	15 (5.99e0)	13 (5.19e0)	13 (5.15e0)
32	29 (2.37e1)	20 (1.22e1)	18 (8.97e5)	15 (7.52e0)	14 (6.55e0)
64	41 (4.52e1)	26 (2.23e1)	22 (1.56e1)	19 (1.32e1)	18 (1.03e1)
128	58 (8.85e1)	36 (4.25e1)	30 (2.88e1)	25 (2.23e1)	23 (1.82e1)
256	80 (1.75e2)	50 (8.83e1)	41 (5.57e1)	34 (4.24e1)	31 (3.42e1)
16	367 (3.64e4)	248 (1.10e4)	187 (6.78e3)	19 (6.78e0)	17 (5.73e0)
32	525 (7.47e4)	326 (2.32e4)	252 (1.32e4)	22 (9.33e0)	19 (7.74e0)
64	740 (1.51e5)	458 (4.76e4)	329 (2.72e4)	28 (1.70e1)	22 (1.25e1)
128	1062 (3.05e5)	665 (9.62e4)	457 (5.52e4)	38 (3.15e1)	29 (2.25e1)
256	1522 (6.12e5)*	980 (1.94e5)*	679 (1.11e5)*	52 (6.06e1)	41 (4.28e1)
16	288 (9.43e3)	98 (5.46e3)	29 (1.60e1)	23 (9.60e0)	21 (6.54e0)
32	443 (1.97e4)	129 (1.14e4)	38 (2.75e1)	28 (1.53e0)	23 (8.00e0)
64	612 (4.03e4)	170 (2.31e4)	51 (5.07e1)	36 (2.73e1)	29 (1.27e1)
128	856 (8.17e4)	232 (4.65e4)	70 (9.82e1)	48 (5.20e1)	38 (2.26e1)
256	1207 (1.64e5)	315 (9.33e4)	98 (1.94e2)	66 (1.02e2)	52 (4.30e1)

* Stagnation.

Table 3 Top: $\alpha = 1$. Middle: Distribution of α from Figure 1 with $\hat{\alpha} = 10^4$. Bottom: Distribution of α from Figure 2 with $\hat{\alpha} = 10^4$. Iteration count and condition number estimate for the classical multiscale coarse space and SHEM_m, $m = 1, 2, 3, 4$, solving Problem 1 for decreasing h, $H = \frac{1}{8}$ and overlap $\delta = 2h$.

3.2 What is the condition number growth in H/h?

We now test numerically the dependence on the mesh ratio H/h for the case where $\alpha = 1$ and for the high contrast cases given in Figure 1 and 2 with $\hat{\alpha} = 10^4$. The iteration counts and condition number estimates are given in Table 3 for decreasing h while the subdomain diameter is kept fixed at $H = 1/8$. We clearly see that the convergence rate is linearly dependent on the mesh ratio H/h, for both the constant coefficient case and the high contrast cases. This confirms that the restrictions in the analysis in [9] are not a property of SHEM itself, but rather restrictions of the analysis. We also see that for very high contrast, SHEM can even fix stagnation when using the appropriate amount of enrichment.

4 Conclusions

The numerical experiments we presented indicate that the first convergence estimate for SHEM in Theorem 1 might not need the technical assumption of small overlap, and also that the convergence bound with the square dependence on the mesh ratio H/h is too pessimistic. Another important observation is that the dimension of the coarse space is not larger than the

dimension of the largest subdomain in our experiments, and thus the coarse space solve remains less expensive than the subdomain solves. Based on this numerical investigation, we are currently carefully studying the technical estimates in the proof of Theorem 1 to see under which conditions on the high contrast parameter α the overlap restriction and the quadratic dependence on the mesh ratio in the condition number estimate can be removed. We are also working on the extension to three dimensional problems, see [2], and on a parallel implementation.

References

1. Jørg Aarnes and Thomas Y. Hou. Multiscale domain decomposition methods for elliptic problems with high aspect ratios. *Acta Math. Appl. Sin. Engl. Ser.*, 18(1):63–76, 2002.
2. Erik Eikeland, Leszek Marcinkowski, and Talal Rahman. Overlapping Schwarz Methods with Adaptive Coarse Spaces for Multiscale Problems in 3D. *arXiv:1611.00968*, November 2016.
3. Martin J Gander and Laurence Halpern. Méthodes de décomposition de domaine. *Encyclopédie électronique pour les ingénieurs*, 2012.
4. Martin J. Gander, Laurence Halpern, and Kévin Santugini Repiquet. Discontinuous coarse spaces for DD-methods with discontinuous iterates. In *Domain Decomposition Methods in Science and Engineering XXI*, pages 607–615. Springer, 2014.
5. Martin J. Gander, Laurence Halpern, and Kévin Santugini Repiquet. A new coarse grid correction for RAS/AS. In *Domain Decomposition Methods in Science and Engineering XXI*, pages 275–283. Springer, 2014.
6. Martin J. Gander, Laurence Halpern, and Kévin Santugini Repiquet. On optimal coarse spaces for domain decomposition and their approximation. In *these proceedings (submitted)*. 2017.
7. Martin J. Gander and Atle Loneland. SHEM: An optimal coarse space for RAS and its multiscale approximation. In *Domain Decomposition Methods in Science and Engineering XXIII*. Springer, 2016.
8. Martin J Gander, Atle Loneland, and Talal Rahman. Analysis of a new harmonically enriched multiscale coarse space for domain decomposition methods. *arXiv preprint arXiv:1512.05285*, 2015.
9. Martin J. Gander and Bo Song. Complete, optimal and optimized coarse spaces for AS. In *these proceedings (submitted)*. 2017.
10. I. G. Graham, P. O. Lechner, and R. Scheichl. Domain decomposition for multiscale PDEs. *Numer. Math.*, 106(4):589–626, 2007.
11. A. Heinlein, A. Klawonn, J. Knepper, and O. Rheinbach. Multiscale coarse spaces for overlapping Schwarz methods based on the ACMS space in 2d. *ETNA*, page submitted, 2017.
12. Axel Klawonn, Patrick Radtke, and Oliver Rheinbach. Feti-dp methods with an adaptive coarse space. *SIAM Journal on Numerical Analysis*, 53(1):297–320, 2015.
13. Nicole Spillane, Victorita Dolean, Patrice Hauret, Frédéric Nataf, Clemens Pechstein, and Robert Scheichl. Abstract robust coarse spaces for systems of PDEs via generalized eigenproblems in the overlaps. *Numerische Mathematik*, 126(4):741–770, 2014.